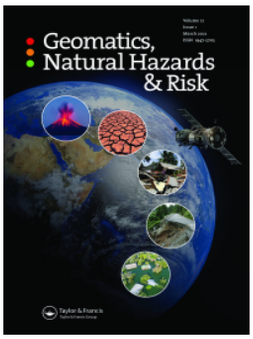

Geomatics, Natural Hazards and Risk

ISSN: (Print) (Online) Journal homepage: https://www.tandfonline.com/loi/tgnh20

Application of a multi-hazard risk assessment for local planning

Kyle D. Buck & J. Kevin Summers

To cite this article: Kyle D. Buck & J. Kevin Summers (2020) Application of a multi-hazard risk assessment for local planning, Geomatics, Natural Hazards and Risk, 11:1, 2058-2078, DOI: 10.1080/19475705.2020.1828190

To link to this article: https://doi.org/10.1080/19475705.2020.1828190

GEOMATICS, NATURAL HAZARDS AND RISK
2020, VOL. 11, NO. 1, 2058–2078
https://doi.org/10.1080/19475705.2020.1828190

Taylor & Francis
Taylor & Francis Group

Application of a multi-hazard risk assessment for local planning

Kyle D. Buck and J. Kevin Summers

US EPA Office of Research and Development, Gulf Breeze, FL, USA

ABSTRACT

Multi-hazard assessments are increasingly vital to communities as exposures continue to change. Their data can provide a nuanced understanding of hazard interactions and their contribution to risk reduction. In previous work, the Patterns of Risk using an Integrated Spatial Multi-Hazard (PRISM) approach produces composite measures of vulnerability and risk at the county level for this purpose. The approach has the flexibility to be applied at a local level to benefit hazard vulnerability assessments and community sustainability planning activities. In this article, we use U.S. census tracts as proxy for neighbourhoods for a localized PRISM approach. The goal is to demonstrate the applicability of the PRISM approach at the community level and identify vulnerabilities in social, cultural, economic, and built systems for use in comparative analyses and mitigation planning. Exposure estimates are created using spatial extents and modelled data from 12 natural and 4 technological hazards. Land area, population counts, and property values are used to estimate vulnerability. National patterns of exposure, vulnerability, and risk reveal distinct regional trends that point to the importance of how impacts are defined. Eight case study examples demonstrate how the data can be analyzed to compare drivers of community vulnerability and risk.

ARTICLE HISTORY
Received 3 March 2020
Accepted 21 September 2020

KEYWORDS
Risk; exposure; multi-hazard; spatial; community; census tract

1. Introduction

The hazard landscape, or 'hazard-scape' is inherently complex, and grappling with the myriad of new and intensifying hazards in a comprehensive manner thus requires some form of model by which exposures are tallied and assigned to locations (Cutter et al. 2010). For local planning purposes, communities need hazard exposure estimates at a meaningful scale to assess risk to people, property, and infrastructure. Two challenges make useful data acquisition difficult. First, data quickly becomes obsolete as hazards rapidly change in intensity, location, and occurrence intervals. Second,

CONTACT Kyle D. Buck Buck.Kyle@epa.gov

most communities encounter a combination of hazards with varying geographic scales and impacts.

Shifts in the hazard-scape and an ever-increasing exposure burden (owing to population growth and movement to high-hazard locations) confirm the importance of maintaining a current and comprehensive hazard risk assessment. According to the United Nations 2015 report on the human cost of weather-related disasters, the global increase in hazard exposures from 1970 to 2010 was between 114 and 192 percent, depending on the hazard. These exposures resulted in over 1.1 million deaths and $1.3 trillion in property losses, with an additional 2.7 billion people adversely impacted in that same time (Wahlstrom and Guha-Sapir 2015). As populations continue to grow, urbanize, and shift into areas with greater exposure potential, the impact of continually intensifying hazards will only continue to grow (Chester et al. 2000; Lall and Deichmann 2012; Garschagen and Romero-Lankao 2015; Güneralp et al. 2015).

Multi-hazard assessments at the county level are helpful in many respects, including a more nuanced understanding of hazard interactions and their contribution to risk reduction (Hewitt and Burton 1971; Kappes et al. 2012). This shift in conceptualization has helped shape risk assessments and provided a means to account for the complex interaction of hazards caused by natural, societal, and technological events (Cutter and Solecki 1989; Cutter 1996). Examples of evolving hazard integration approaches are evident in research using spatial tools for loss estimation, planning and mitigation purposes (Batista et al. 2004; Fleischhauer et al. 2005; Greiving et al. 2006; Schmidt-Thome 2006; Tate et al. 2011; Federal Emergency Management Agency (FEMA) 2009a). The Patterns of Risk using an Integrated Spatial Multi-Hazard (PRISM) approach tackles the challenge of providing a multi-hazard risk assessment across multiple spatial and temporal scales while also retaining a more integrative assessment of risk (Buck et al. 2019). The complexity of natural systems, and to some extent the human systems, is addressed using county level assessments of risk.

The utility of the PRISM approach was demonstrated at the county level and included as the basis for a Natural Hazards Resilience Screening Index (Summers et al. 2018). In that application, hazard exposures were weighted by land cover and analyzed in conjunction with the social, economic, built, and political environments to make assessments and recommendations to county, state and regional officials. Moving forward it is important to recognize the pivotal role of local planning and mitigation activities in addition to the larger efforts. The PRISM approach is easily adapted to create exposure estimates at the local and community level and would supply consistent data for planning and mitigation purposes. Hazard mitigation is an important component in sustainable development in community planning and requires information to define hazard zones (Cutter et al. 2008). The vulnerability of U.S. populations has continued to increase as people move to urban areas within hazard zones. Even so, the increase in vulnerability is not evenly distributed within counties cities.

Vulnerability assessment is a central component of sustainability planning and includes hazard identification along with an accounting of social, cultural, economic, and built systems impacted (Mileti 1999; Burby 2000). Application of the exposures, or hazard surfaces, created in the original PRISM to these local systems will create

useful data to track changes and plan for future development. Most land-use actions are guided by the characteristics of the underlying data in hazard mitigation planning. The original PRISM work used land cover data as a proxy for land-use to quantify vulnerability weighted by the extent of rural and urban environments. In a local vulnerability assessment, hazard exposure probabilities by land use could guide decisions regarding new development. Using population data, a vulnerability assessment would help quantify human risk and inform evacuation planning and potential needs post disaster. Similarly, parcel data would aid loss probability estimates for infrastructure and buildings. New building codes and system improvements are often driven by these assessments. In each of these examples, only the underlying, or exposed, surface requires changing to produce vulnerability assessments.

The goal of this article is to demonstrate the applicability of the PRISM approach at the community level and identify vulnerabilities in social, cultural, economic, and built systems for use in sustainability planning. Hazard exposure layers from the original PRISM work are applied to population, land cover, and household data to create vulnerability estimates. In addition to providing a practical demonstration of the land-use vulnerability assessment at the community level, the research presented here also proposes a theoretical basis to add the socioeconomic and cultural dimensions to a multi-hazard assessment. The information generated in this study provides practical insight with respect to evacuation challenges, mitigation planning, and recovery metrics that would be useful to city planners and allow for consistent tracking through time.

2. Methods

This work is an application of the PRISM framework using original hazard extents and replacing counties with census tracts as the aggregation units for exposure. A brief overview of the PRISM framework's methods and conceptual underpinnings are covered first. In the tract-level application of the framework, there are three exposed biophysical attributes examined: land area coverage, population counts and property values. The final part of the research involves the use of national and case study summaries to describe relationships between each exposure measure and vulnerability.

2.1. Original PRISM framework

The PRISM framework is built using a place-based conceptualization of hazard exposure that assesses eleven natural hazard types. Eight of these are assessed using historic events. Points, areas or tracks of each hazard are collected for each hazard and georeferenced. For hazards with defined spatial boundaries, further processing is carried out to estimate the extent of potential exposure (e.g., tornado path width, hurricane wind field). A spatial overlay analysis is used to estimate proportional exposure within each county by land-use proxy (natural, dual-use, and developed) derived from the National Land Cover Database (NLCD) (Homer et al. 2015). In addition to historic hazard exposures, the original PRISM approach assesses proximity-based exposures based on location in relation to potential hazards. Locations with a

Table 1. Hazard Exposure Calculations for 11 natural hazard types used in original PRISM method and applied to census tracts (King and Beikman 1974; Simpson and Reihl 1981; Radburch-Hall et al., 1982; Weatherford and Gray 1988; USGS 2003; Brooks 2004; Zhu 2008; FEMA 2009a; FEMA 2009b; FEMA 2013; NWS 2016; NWS 2018; Hawbaker et al. 2017).

Natural hazard type	Class	Spatial extent	Exposure calculation
Hurricane	Historic and Modelled	Buffer of 100 miles surrounding tracks for storms > Category 1.	Proportion of each land-use classification used to estimate exposure extent.
Tornado	Historic and Modelled	Adaptive buffer based on path width data and mapped tornado tracks.	Proportion of each land-use classification used to estimate exposure extent.
Earthquake	Modelled w/Historic	USGS Modelled data -historic events and probability of event exceeding 0.1 g PGA.	Proportion of each land-use classification used to estimate exposure extent.
Fire	Historic	Ignition sites of historic fires with adaptive buffer using total burn acreage.	Proportion of each land-use classification used to estimate exposure extent.
Drought	Historic	U.S. Drought monitor database extents for 5-year period in two categories (D3-D4)	Proportion of each land-use classification used to estimate exposure extent.
Wind	Historic	Entire county used as extent.	Avg. number of damaging wind events (>50 mph) per year within the county.
Hail	Historic	Entire county used as extent.	Avg. number of damaging hail events (0.75″) per year within the county.
Landslide	Modelled w/Historic	USGS historic landslide incidence and susceptibility based on slope and terrain types.	Proportion of each land cover classification used to estimate exposure extent.
Temperature Extremes (high and low temp. deviations)	Historic	Entire county used as extent.	The avg. deviation of annual min and max val. from the 32-year average high and low temps.
Inland flood	Modelled	0.5-mile buffer around inland waterways (rivers, streams, lakes, ponds, etc.)	Proportion of each land cover classification used to estimate exposure extent.
Coastal flood (Sea level rise/storm)	Modelled	Buffer along all coastal counties for land within 2 ft of current sea level at mean high tide.	Proportion of each land-use classification used to estimate exposure extent.

potential for hurricane, tornado, and flood exposure (e.g., located on coastal waters, in tornado-prone area, etc.) are assigned a proximity-based probability if they fall within an area with future exposure potential. Technological hazard exposure probabilities are calculated using buffers around hazard sites. Areas within buffers are assigned a probability based on the hazard type. Tables 1 and 2 provide a summary of the calculations used to create spatial exposure measures for all natural and technological hazards.

Losses in the original PRISM approach are combined into three categories: built, dual-benefit, and natural, represented by loss data on property, crops, human lives, and natural land conversion. This conceptualization of vulnerability is couched in the place-based assessment paradigm where it represents both a biophysical exposure and a social response (Blaikie and Brookfield 1987). Using losses in this capacity provides a context for the level of risk based on harms incurred as a result of exposure (Cutter

Table 2. Hazard exposure calculations for 4 technological hazard types used in original PRISM method (Batista et al. 2004; USNRC 2014).

Technological hazard type	Spatial extent	Exposure calculation
Nuclear facilities	All nuclear reactors and storage facilities in U.S. identified and given a 10-mile buffer.	Proportion of each land cover classification used to estimate exposure extent.
Superfund sites	Superfund sites – proposed or active in the U.S. identified and given a 5-mile buffer.	Proportion of each land cover classification used to estimate exposure extent.
Toxic Release Inventory (TRI) Sites	TRI facilities identified when threshold chemical release criteria are met and given a 1/4-mile buffer.	Proportion of each land cover classification used to estimate exposure extent.
Resource Conservation and Recovery (RCRA) Sites	All RCRA Site (LQGs, TSDs, and TRANSs) point data from EPA FRS Geodatabase are given a 1/4-mmile buffer.	Proportion of each land cover classification used to estimate exposure extent.

1996). We are measuring the outcome of hazard incidences across a landscape and therefore are considering the losses only in this context.

2.2. Scaling PRISM to the census tract

The application of PRISM described here uses the same multi-hazard spatial exposure framework but replaces county land-use values with census tract land area, population counts and property values as the exposed surfaces. Census tract geographies are useful in the evaluation of population and other socioeconomic variations within a community and serve as a proxy for neighbourhoods (U.S. Census Bureau 2015). While they represent populations larger than the typical suburban neighbourhood, there is still a strong association between the spatial extent and population count that makes them useful in hazard exposure assessment (e.g., areas of high population density will have smaller tract extents). The original spatial extents and temporal scale (2000–2015) for natural and technological hazards are utilized to create exposure estimates (Tables 1 and 2). Population and property value estimates are based on 2015 Census data (U.S. Census Bureau 2015) and used to estimate vulnerability. County-level loss data is used with the tract-level vulnerability estimate to create the final risk estimates.

The exposure extent estimates for each hazard type are merged to create a tract-level proxy for multi-hazard exposure probability. Equation (1) shows the calculation used to derive tract-level exposure scores, where E_h is the historic and modelled hazard exposure, E_p is the proximity-based exposure, and E_t is the technological exposure.

$$Exposure = \left[\sum E_h + \sum E_p\right] X \left[\sum \left(\frac{E_t - E_{tmin}}{E_{tmax} - E_{tmin}}\right) + 1\right] \quad (1)$$

The historic and modelled hazard exposures are summed first and account for one of three exposure types (Table 1). Those hazards with defined spatial boundaries are calculated as land area proportions, which are summed to create the score for this

index component (E_h). Proximity-based exposures are assigned an exposure value due to location (e.g., coastal tracts along the Southeast Atlantic have an inherent hurricane risk even if not hit by storm in past 16 years). These exposures include the proximity-based estimations of hurricane exposure, tornado exposure, inland flood exposure, and coastal flood exposure. They are summed independently of the spatially referenced historical exposures, with the exception being hurricanes and tornados. Each of these hazards are calculated as a combination of proximity based and historic exposures. In the cases where the total exposure proportion exceeds 1, the values are constrained.

The third and final exposure classification is associated with technological hazards (Table 2). These are included in the model to represent the intersection of contaminated sites, human populations, and natural hazards. Reduction of losses and improved community resilience can be improved through effective emergency management, which requires knowledge of these potential intersections (Durham 2003). Technological hazards are summed, and the resulting values standardized, then constrained between 1 and 2. This is done to account for the exacerbation of threats when natural and technological hazards coincide and the capacity of a place to handle the combination of hazard events. The risk of a secondary event will be greater in a place with higher numbers of contaminated sites. Since the technological hazard score is multiplied by the natural hazard score, tracts with no technological hazard exposures will retain their original value (natural hazard exposure only), while tracts having the highest technological exposures could potentially double their natural hazard score.

There are a few minor changes made to the original hazard surface calculations that should be noted. Drought exposure is measured using only the D3 and D4 (moderate and severe) classifications. This is done to increase variance in exposure extents. Using the 16-year pooled data for all drought categories (i.e., D1–D4) resulted in one hundred percent tract coverage (NDMC 2017). The second modification is made to Resource Conservation and Recovery Act (RCRA) sites. In the original PRISM index, RCRA was calculated using ¼ mile buffer surrounding sites. There are, however, a relatively small number of sites, and the overlap of census tracts is small enough to be insignificant. In order to retain the information and comparability between county and tract indices, the RCRA sites are assigned to counties and the counts are min-max standardized for inclusion in the index. The third and final change is made to the coverage extent for the final maps, which now covers only the contiguous U.S. This is due to: (1) significantly lower risk scores and little variability across both Alaska and Hawaii, (2) sparse population across most of Alaska, and (3) the island geographies of Hawaii with few hazards. In addition to these changes, there are some hazard extents remain at a county scale due to data limitations. These include high wind events, large hail events, and extreme temperature (high and low deviations) events. For these hazard types, the county exposure value is attributed equally across all census tracts within its boundaries. This is expected to result in loss of variance at the tract level and could be supplemented in local analysis with available data. As better spatial data becomes freely available, calculation of these metrics would be worthwhile on a national scale.

Tract-level vulnerability estimates use the multi-hazard exposure probabilities to reveal where land, population, and buildings are most likely to intersect with hazards and create vulnerability. Higher probabilities, both in extent and number of hazard-type exposures, will increase the vulnerability, or likelihood of harm. Population and property vulnerability estimates are attained by first calculating the proportional overlay of natural hazard extents and census tract boundaries. This serves as the multi-hazard exposure layer. Population vulnerability is calculated by multiplying tract-level population estimates by the multi-hazard exposure values (for those hazards with defined extents). Hazards using this calculation method are hurricanes, tornadoes, wildfires, droughts, landslides, earthquakes, inland floods, coastal floods, superfund sites, nuclear sites, and TRIs. Property vulnerability estimates are created using the same method. First, tract-level household counts are multiplied by the median household value estimates to create a total property value in each tract. This measure is multiplied by the multi-hazard exposure values to create an estimate of property vulnerability. Local studies could use parcel data to get household counts and value estimates for a more accurate estimate of vulnerability.

The PRISM framework estimates risk through the incorporation of loss estimates to represent the intensity and impact of hazards to the landscape. Risk, in this conceptualization, is represented by the vulnerability combined with associated losses. Loss data comes from the Hazard and Vulnerability Research Institute's (HVRI) Spatial Hazard Events and Losses in the U.S. (SHELDUS) database and is available at the county level for property (year adjusted dollar total), crops (year adjusted dollar total), human lives (total number), and injuries. SHELDUS losses are population weighted, averaged in 5-year segments. Natural losses are assessed using NLCD land cover change data, which identifies land cover pixels that have changed to impervious surfaces (indicating built environment) between 2001 and 2016. The percentage of land in a census tract converted to the built environment is used as a proxy for natural land lost. Damage posed to natural systems resulting from population stresses or other anthropogenic influences, represented by the natural land loss, foreshadows potential reductions in ecosystem services (Hey and Philippi 1995).

The loss categories (property, crop, human and natural) from PRISM are generated and combined at the tract level for this application. The individual loss category values are retained for analysis, however final tract-level risk calculations are completed using combined loss estimates. The loss score is scaled (1–2) and used as a multiplier to estimate risk. This retains a final score (vulnerability $\times$ loss) representative of inherent tract-level risk given the exposures. Unfortunately, county level estimates must be used here due to a lack of data at smaller aggregations. In local applications, this data may be available and used to supplement and improve the county-level loss estimates.

Three tract-level datasets are created from these applications: (1) a land cover vulnerability and risk estimate at the tract level (most consistent with the original PRISM approach), (2) a population vulnerability and risk estimate using census tract population estimates, and (3) a property vulnerability and risk estimate using census tract residential property value estimates. Regional patterns of vulnerability and risk are analyzed along with specific hazard exposures driving each of these.

Five urban case study sites (Atlanta, GA; Houston, TX; Seattle, WA; Chicago, IL; and Denver, CO) and three rural sites (Kendall County, IL, Polk County, TX, and San Benito County, CA) are chosen from around the U.S. to show local patterns and demonstrate the utility of PRISM to community vulnerability and risk assessments. The urban sites are exposed to a wide variety of hazards and have very different population profiles. In addition, they are among the fastest growing cities in their regions. The rural sites are chosen for their proximity to urban areas, agricultural importance within their state, and distinct hazard profiles. Each of these locations face complex decisions to best incorporate hazard mitigation into their sustainability plans. Profiles of land cover, population and property vulnerability show clear patterns of disparity and help prioritize mitigation action. In rural areas outlying a large urban center, these patterns would also help with approaches to new land development as the population continues to rise. Both scenarios are discussed along with examples of data produced from the model. This exercise both provides validation of the framework and a use case for creating local level risk estimates for planning.

3. Results

Maps are created first to analyze spatial patterns of the three vulnerability datasets. These are produced at the tract level for the contiguous U.S. and shown as a panel with land, human, and property vulnerability scores for 2015 census tracts (Figure 1). Each map displays multi-hazard vulnerability based on multi-hazard exposures from 2000 to 2015 modelled and historic data.

The patterns of vulnerability are spatially distinct. Land area vulnerability is focussed primarily in the Southeast along the coasts and in a large swath of the Great Plains states. The human and property vulnerability maps utilize land area proportional coverage to better illustrate where the highest concentrations of people and residential values intersect with hazard exposures. Human vulnerability, like land, highlights areas along the Southeast coast. Instead of the Great Plains, however, there are more high vulnerability population clusters in the Midwest. There is a distinct lack of population vulnerability in the Western U.S. Residential property vulnerability has fewer large clusters of high scores. Most areas of high vulnerability are found in the large urban core of the Northeast (around New York city) along with some clusters surrounding coastal urban areas in Florida, Texas, and California.

To get a sense of the hazards driving vulnerability in the tracts, a table is created to show all hazard contributions as percentages of total exposure (Table 3). The leading hazards are related to extreme temperatures and thunderstorms (high wind and hail), contributing to greater than 95% of all tract exposures.

Contributions of individual hazards to tracts with the highest land, population, and property vulnerability are shown in Figure 2. For each chart, hazard data represents tracts with vulnerability scores greater than one standard deviation over the mean. This results in 13,036 tracts with high land vulnerability, 11,696 tracts with high population vulnerability, and 9,409 tracts with high property vulnerability. Exposures driving the property vulnerability chart are limited to only those hazards capable of damaging structures. This eliminates extreme temperatures and drought

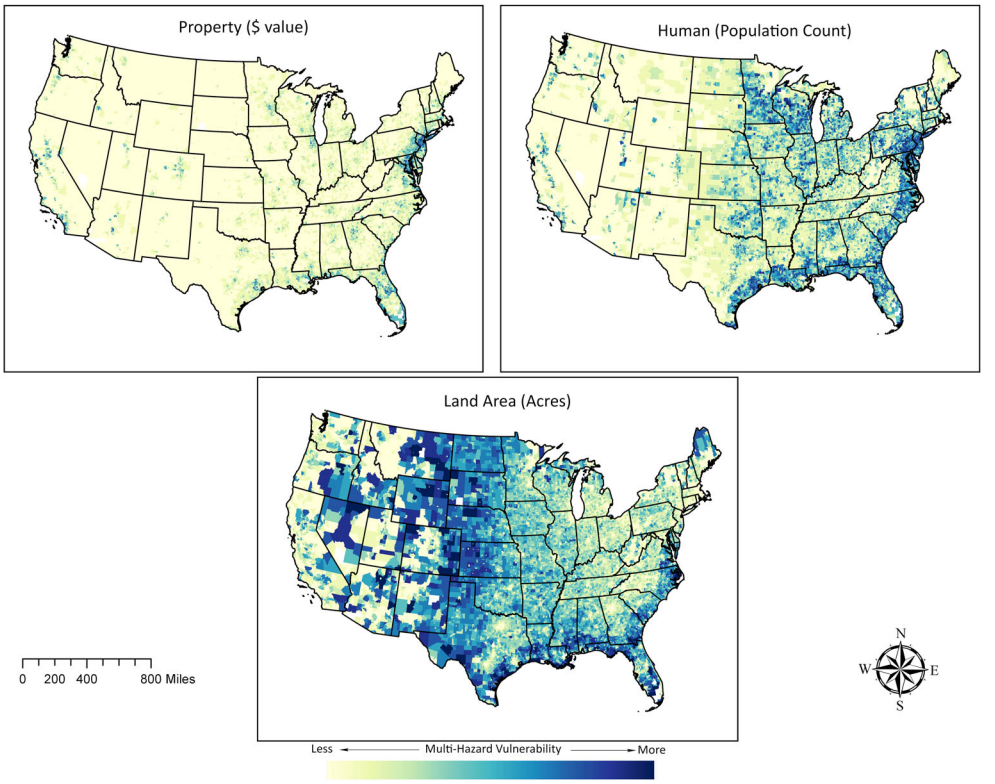

Figure 1. Three panel map showing multi-hazard vulnerabilities at the tract level in 2015. The land area vulnerability map represents the proportion of each tract with exposure to hazards. It represents a baseline and is used the calculate the other two vulnerability estimates. The property vulnerability map is based on total residential property value exposed (inflation-adjusted $), calculated as the number of households multiplied by the median household value and land proportion exposed to hazards. Human vulnerability is based on the total population exposed, calculated as total tract population multiplied by the land proportion exposed to hazards.

from the chart. Comparing the tract exposures from Table 1 to the highest vulnerability tracts in Figure 2, the distributions are not significantly different. Hazard exposures driving the most land and population vulnerability remain extreme temperatures, wind, and hail. Property vulnerability is primarily driven by wind and hail.

The spatial distribution of land, population, and property risk is shown in another map panel (Figure 3). Like land vulnerability, land risk is high along coastal counties in the Southeast. There is, however, a noticeable shift from the rural Great Plains states to numerous large urban clusters in the Eastern U.S. Population and property risk both retain patterns similar to vulnerability. Higher population risk clusters appear throughout the Southeast coastal regions and in the Midwest. Property risk remains lower across the country. Like property vulnerability, corresponding risk scores cluster around New York, NY, much of Florida, and some coastal areas is Texas and California.

Table 3. Individual hazard contributions to tract-level vulnerability from 2000 to 2015.

Hazard	% Contribution
Ext. high temps	39%
Ext. low temps	31%
High wind	16%
Hail	9%
Coastal flood	2%
Tornado	1%
Earthquake	0.62%
Hurricane	0.44%
Inland flood	0.19%
Fire	0.17%
Drought	0.12%
Landslide	0.00%

2010 tract boundary files and 2015 ACS 5 yr estimates used for all U.S. contiguous U.S. tracts.

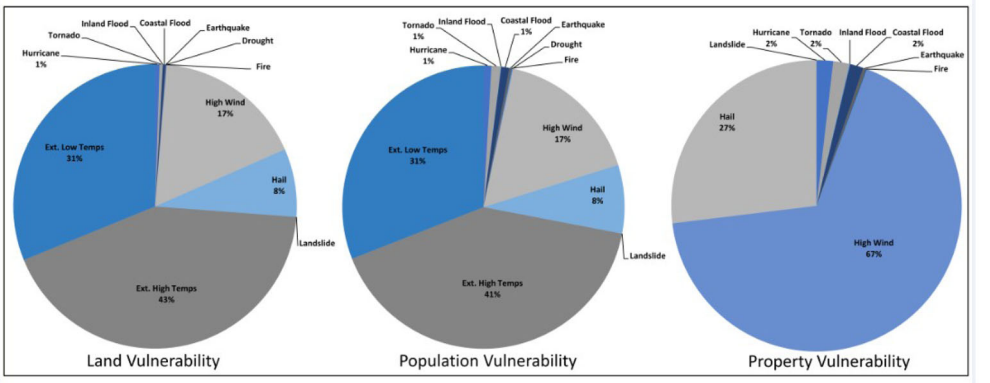

Figure 2. Pie charts showing the natural hazards contribution to vulnerability scores. Data represents the most vulnerable tracts from each of the three datasets (land area, population, and property). Most vulnerable tracts selected as those with scores greater than 1 standard deviation above the mean for all tracts. Note: Property vulnerability does not include extreme temperature or drought exposures. These hazards are not associated with structural damage or loss.

The number of hazard exposure-types occurring within tract boundaries over the 16-year timespan is important to consider as a driver of vulnerability in this analysis. The analysis includes all hazard types with available spatial extents; a total of 11 hazard types. Distribution of total hazard-type exposures is shown in Figure 4. Patterns in this map indicate more exposures are present in the Southeast and Western states, which corresponds only to areas of higher population vulnerability and risk. Areas with low hazard-type counts are primarily in the Northeast and Great Lakes as well as in some parts of the Southwest. Few areas exist that do not have some combination of hazard types, and even fewer have no exposures. The maximum number of hazard-types present in any of the tracts is 11, and the mean is just under 4 (3.929). Only 209 tracts of the 72,320 analyzed with no hazard-type exposure, which suggests that most U.S. Tracts are exposed to multiple hazards and should consider mitigation strategies accordingly.

In addition to having utility at the national level, a nationally consistent tract-level vulnerability and risk analysis can be useful to local preparedness evaluations and mitigation activities. To demonstrate this, we conduct eight case studies across the

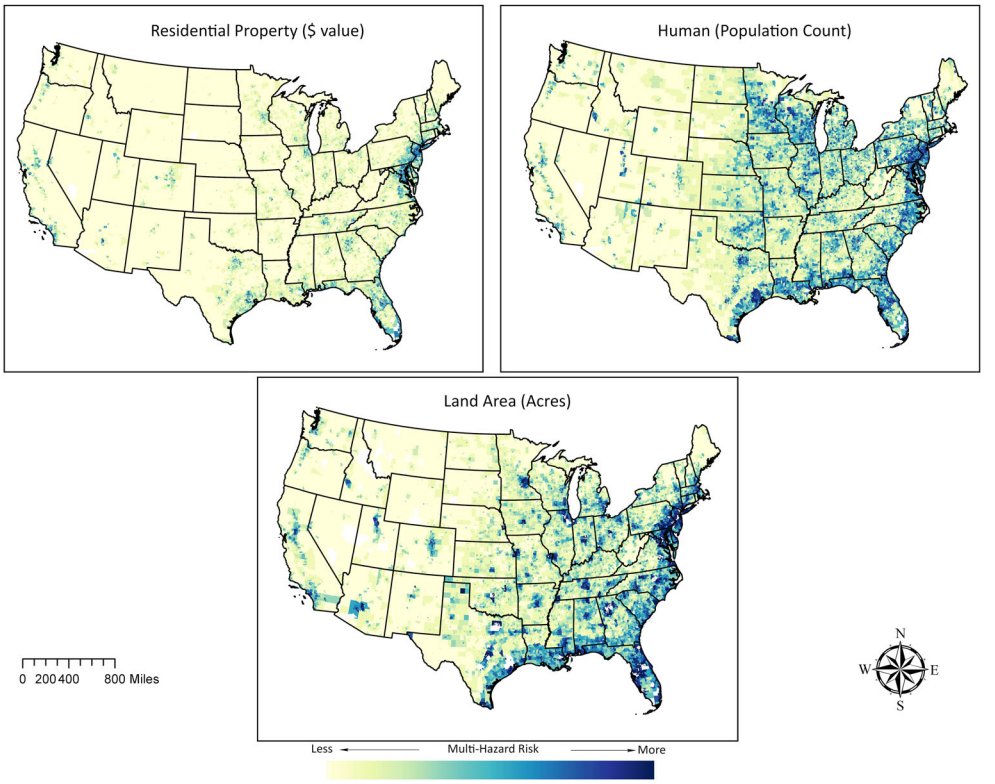

Figure 3. Three panel map showing multi-hazard risk at the tract level in 2015. The land area risk map represents the tract land vulnerability multiplied by the total county hazard losses. The property risk map is based on residential property vulnerability multiplied by the county level property losses. Human risk is based on the human vulnerability multiplied by the county estimates of lives lost to natural hazards.

U.S that encompass urban and rural communities with distinct hazard profiles. The map in Figure 5 shows locations and insets of population risk data for each of the sites.

Each of the case study map insets are based on the same scale, which is beneficial for comparison. Looking at the urban case studies, the average scaled population risk score for Houston (0.16) is significantly higher than the overall tract mean (0.07). Atlanta (0.08) and Denver (0.08) are both just over the risk mean, while Chicago (0.05) and Seattle (0.02) each fall well below. The rural sites of Kendall and Polk County each have population risk values just over the mean (0.10 and 0.09, respectively), while San Benito county falls well below the mean (0.01).

The hazard exposure profiles can also be analyzed at a local level for each of the locations. Figure 6 provides a display of the relative hazard exposures. Similar to U.S. trends, temperature extremes have the greatest overall impact. Chicago is the only location where this is not the case. Other locations range from minimal exposure to other hazards to multiple additional exposures. In these cases, wind and hail are the only hazards to have greater than 10% exposure probability.

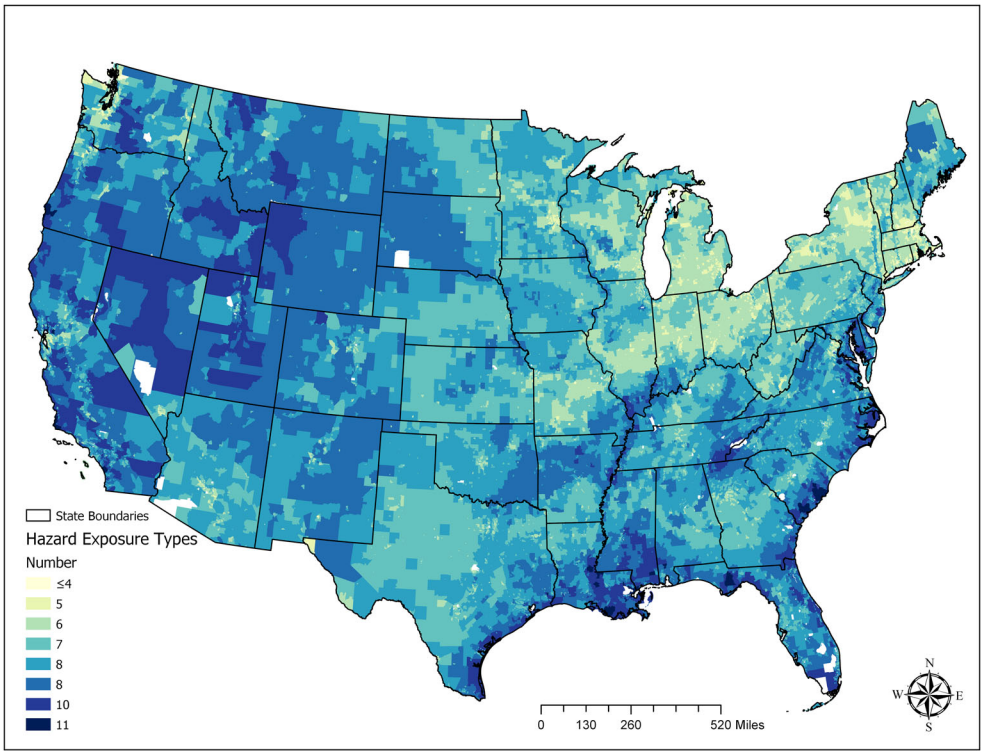

Figure 4. Map showing number of hazard exposure types in each tract from 2000 to 2015.

Putting this information into the context of a comparative risk study, the case study locations of Chicago and Houston are discussed briefly to provide more detail. A community risk analysis in this case will follow the data, starting with exposures before examining what is impacted and potentially harmed as a result. Looking first at exposures, Houston and Chicago have similar hazards types (wind, hail, extreme temperatures) contributing to their risk profiles (Figure 6). Each location has relatively high wind and hail exposures, but Chicago has lower temperature exposures. Despite similar hazard profiles, Chicago has considerably less proportional land exposure when taking all hazards into account (0.31). Houston has over twice the tract mean multi-hazard exposure score (0.64). This can be explained by the presence of more hazard types along with greater exposure to high-loss events. Whereas Chicago is exposed to only eight hazard types, Houston is exposed to 11. Houston also has relatively high probability of exposure to hurricanes, tornados and flooding (inland and coastal). Each of the hazard types is associated with high loss and Chicago has effectively zero exposure to any of them (Tornado and Coastal Flood = 0.0004).

Quantifying population risk requires an estimation of population likely exposed given the hazard occurrences. While Chicago and Houston both have similar population numbers (2.7 million and 2.3 million, respectively), their population distributions are quite different. Chicago has a very dense urban core with just under 12,000 people per square mile. Houston has a much larger footprint, but a density of only 3,800

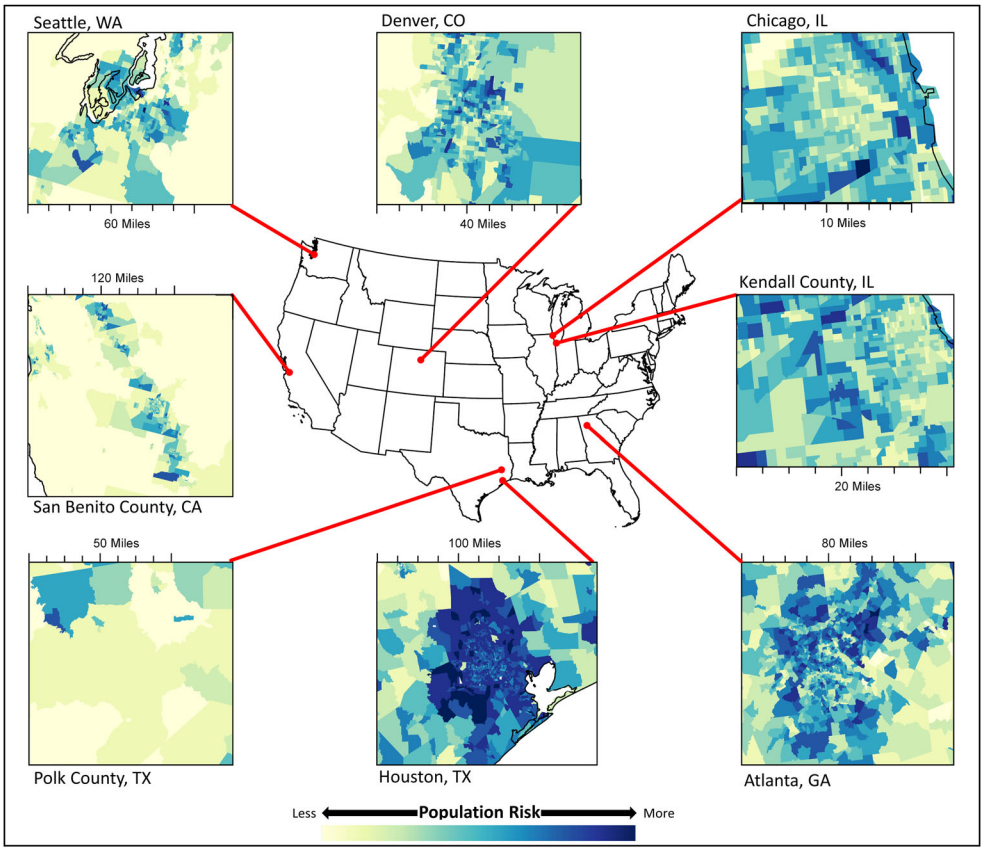

Figure 5. Case study locations and map insets showing population risk data. Eight case study locations are: Seattle, WA, Denver, CO, Chicago, IL, Atlanta, GA, Houston, TX, Polk County, TX, San Benito, CA, and Kendall County, IL.

people per square mile. What this means for risk assessment is complex and requires an ability to look at individual hazards and impacts. The higher density in Chicago will result in higher exposures per tract, but the impact will be more confined. Houston has more exposure potential because of its large spatial extent, but each individual tract will have less. While more compact developments will result in similar exposures to most hazards, the expected vulnerability and impacts are lower (Chang et al. 2019). Between Houston and Chicago, the larger exposure is likely due to the hazard types present in addition to the number of hazard types. Multiple hazard types over Houston's large extent mean tracts in different locations will have numerous and diverse exposures. For instance, tracts near the Gulf of Mexico will contend with coastal flooding and a high hurricane risk while those inland may have high tornado and wind exposure. Given these diverse exposures and wider population distribution, the average population vulnerability in Houston (0.12) is greater than that of Chicago (0.06).

The final risk estimates are created after vulnerability is multiplied by the losses. Houston's overall hazard losses (1.52) are well above the national mean (1.31) while

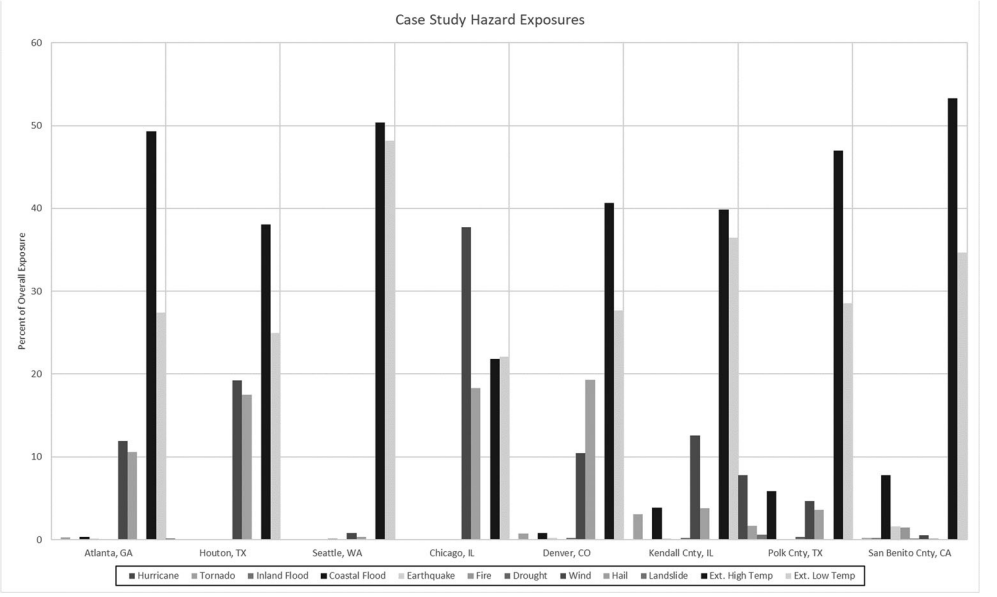

Figure 6. Percent contribution of natural hazards to overall exposure in each of the eight case study sites. Each case study site is shown along the *x*-axis with percent contribution to overall hazard represented by the bar graphs.

Chicago's losses (1.22) are well below. In addition to the inclusive measure, three individual categories of loss provide context for hazard intensity and type. Each of these are measured as either a proportion of county area or population weighted by county. Development losses are nationally low with a mean of 0.0009. Comparatively, both Houston and Chicago have small development losses (0.0001 and 0.00006, respectively), which represent proportional loss of property and lives. This could reflect better mitigation planning that limits damages or loss from hazards. Crop and land losses, combined at the tract level due to their similarity, are the main driver of loss disparities between Houston and Chicago. In Houston, crop and land losses (0.86) are significantly greater than the national mean (0.14), whereas Chicago is slightly below the mean (0.12). Loss of land in Houston is attributed to both heavy development and subsidence, leaving many of the buildings and people more vulnerable (Holzer and Galloway 2005; Kahn 2005). Also, of note, this data is all collected prior to the 2017 landfall of Hurricane Harvey, which inflicted massive damage to the greater Houston area and serves as a prime example of intersecting hazard types and vulnerabilities.

Two major points can be derived from this case analysis. First, the concerns over population influence when using census tracts do not appear to be founded. This was mentioned as a potential issue inherent in the use of census tracts, which are population dependent. If this assumption were to hold true, tracts in population-dense urban areas would account for most hazard exposures. Instead, in the example comparing Houston and Chicago, hazard exposure trends do not mirror population density or tract populations. While Houston's population is largely suburban and

Table 4. Exposure, vulnerability, loss, and risk data for case study locations.

	Urban case study locations					Rural case study locations			
	Houston, TX	Chicago, IL	Atlanta, GA	Seattle, WA	Denver, CO	Kendall Cnty, IL	Polk Cnty, TX	San Benito Cnty, CA	National Mean
Population risk	0.16	0.05	0.08	0.02	0.08	0.1	0.09	0.01	0.07
Multi-hazard land exposure	0.64	0.31	0.31	0.08	0.34	0.2	0.46	0.06	0.31
Population vulnerability	0.12	0.06	0.06	0.02	0.07	0.07	0.11	0.02	0.07
Overall loss	1.52	1.22	1.35	1.29	1.32	1.19	1.24	1.07	1.31
Land/Crop loss	0.86	0.12	0.42	0.06	0.25	0.41	0.01	0.004	0.14
Developed loss	0.0001	0.00006	0.00008	0.001	0.0001	0.00002	0.01	0.0002	0.0009

National mean values included for comparison.

surrounding the urban core, Chicago is very densely populated in the downtown and nearby neighbourhoods, with population falling off towards the periphery. The types of hazards and the loss values have a much larger impact on risk, with values reflecting on the ground observations in these two examples (e.g., Houston's rapid growth and Chicago's notoriety for winter wind and hailstorms). Further local case-studies could help provide more insight.

An examination of the remaining urban sites along with the rural is summarized in Table 4. Chicago and Houston are included as well for comparison. Of the rural sites, Kendall and Polk Counties both have population risks slightly above the national mean. In Kendall, the higher risk is driven primarily by the land and crop loss while Polk has a relatively high multi-hazard exposure score. Both counties are exposed to multiple hazards (Kendal County-8, Polk County-9), but those in Kendall are smaller proportionally. The losses in Kendall are a result of natural land conversion as well as changing rainfall patterns and temperature extremes (O'Keefe et al. 2006). Though it is the fastest growing county in Illinois, Kendall is still primarily rural and reliant on corn and soybean crops. Extreme low temperature events have caused significant losses at harvest time. In San Benito County all measures are well below the national mean. This reflects a rural area with limited residential growth and a diverse agricultural portfolio. While their exposure to extreme temperatures is high relative to other hazard types, it is low nationally. The most significant risks to the county come from fires and earthquakes.

The remaining urban counties of Seattle, Atlanta, and Denver also display different patterns of exposure and risk. For instance, despite having relatively low population risks, both Atlanta and Denver have higher land and crop losses. The cause of this, like that of Houston and Kendall County, is related to natural land conversion. Atlanta and Denver both have rapidly expanding populations that are leading to extensive suburbanization. As this land is converted from natural land to neighbourhoods and shopping centres, the capacity of natural systems is limited, and exposures are increased. Accounting for this type of loss accounts for both the immediate loss of natural and productive habitat and the future benefits these land types confer to the area. Consideration of monetary and life loss alone would not capture this and could subsequently misrepresent the loss in an area.

4. Discussion

National assessments of multi-hazard vulnerability and risk allow for both comparability studies and in-depth assessment of driving influences of risk, thereby addressing two key components that make hazard analysis useful in community-level planning exercises. First, communities with similar characteristics and risk profiles can be grouped for comprehensive analyses of mitigation strategies. Second, the capability to deconstruct risk scores into exposure and loss types permits for a variety of analyses targeted to community goals and resources. It is also possible to analyze these model results in conjunction with policy and economic investments to determine effectiveness of mitigation actions following hazard events.

One important point to make about the PRISM framework in general, and this application specifically, is the flexibility for both comparative analysis and planning purposes. While the visualizations and summary statistics are useful to get an overview of community vulnerability and risk, they are built on a massive amount of information detailing hazard extents and community characteristics. This data is also easily expandable depending on desired analysis. This flexibility is due to the effectiveness of a spatially derived multi-hazard risk analysis like PRISM. Quantifying hazards as proportional land exposures enables them to be combined and assigned to specific geographies. Current applications of PRISM have used census geographies, but proportional exposures just as easily be calculated for any geographic boundary.

In addition to having flexibility in spatial extents and hazard types, there is a choice in how impacts are assessed for vulnerability and risk analyses. National examples are shown here using data for property, population, and land characteristics that are vulnerable to hazards, but these could be expanded to include more specific social, economic, or ecological variables of interest. Changing the characteristics of the impacted area in PRISM to reflect local interests can add utility in mitigation activities. For example, population risk is used in the case study communities here to specifically compare how different hazards may cause harm to people. A similar analysis would look very different if assessing property vulnerability, for instance.

Assessment of property vulnerability, while also important in comparative analysis, has value in development planning and loss prediction. The city of Houston, TX is a useful example of this. In addition to being one of the case studies, it was also hit by a major hurricane shortly after the temporal data range of this work. Hurricane Harvey hit the coast of Texas in August of 2017 and caused $125 billion in damages (FEMA 2018). Specific to this example, high winds, floods, tornados, and hurricane-specific damage resulted in 226,167 individual property claims. Houston is a good example for property damage and planning applications due to its reputation for rapid growth and uncontrolled sprawl that has led to paving over many important wetlands needed for flood control (Berke 2017). Figure 7 shows the vulnerability of census tracts based on the property values (property vulnerability) compared to property claims resulting from Hurricane Harvey. A map like this shows where existing development clearly aligns with losses, confirming the vulnerability. Current flood maps are used to accomplish this for planning and insurance purposes, however, many of the residential damages in Houston were not flood related. Many were far

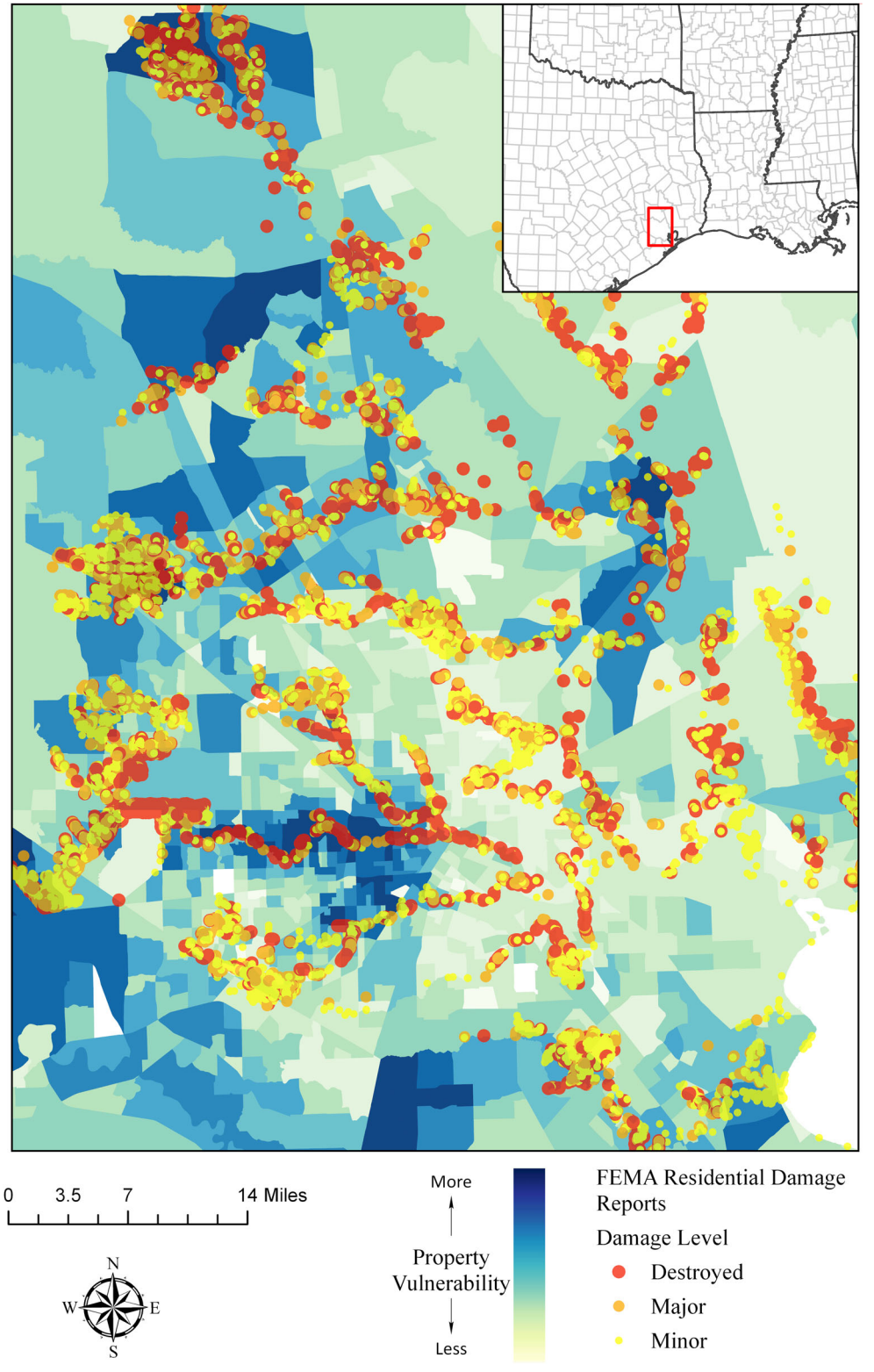

Figure 7. Houston, TX – PRISM values for property vulnerability in 2015 compared to property damage claims from Hurricane Harvey in August 2017.

inland as well, reducing modelled single hazard risk. Multi-hazard modelling allows for comprehensive vulnerability assessments to be created for more accuracy.

Expanding the Houston example, land vulnerability could be assessed in addition to property to make planning decisions. Identifying areas in the city with higher exposures to all hazards would inform insurance decisions and development decisions to reduce future exposures. Population and infrastructure vulnerability in a coastal city like Houston are also important in roadway design for evacuation routes. Multi-hazard exposure can be similarly used with social vulnerability measures to help mitigate loss disparities caused by population characteristics or access. In each of these examples, the same multi-hazard exposure surface is applied to a different set of underlying characteristics in a relatively straightforward process making the explanation and interpretation of results easier.

There are a few weaknesses and areas for improvement as this research moves forward. While most of the hazard types are applied directly to the census tracts, there are several (4 natural hazard types) exposures necessitating use of county data. The impact of this on local variability is unknown, but there would certainly be advantages to calculating local exposures. In addition, loss data at the county level is used directly from the original PRISM approach. With considerable effort, this data could be procured at smaller aggregations for the nation, but locally held loss data for specific communities of interest is a more likely in future applications. To truly represent a local assessment of vulnerability and risk, however, hazard extents and local (tract or smaller) level data will produce the best results and should be sought whenever possible.

The other issue to point out is that of aggregation error, or the modifiable areal unit problem (Fotheringham and Wong 1991). First, all population and property estimates assume even distribution across census tracts. While this may be true for some smaller units in dense urban tracts, it is less likely as density declines and tracts become larger. Estimates of population exposure using aggregation units cannot replace local surveys of exposure. Similarly, the comparison of a census tract risk value both to other census tracts to county risk values will have error introduced by changing the aggregation units (Cheng and Fotheringham 2013). This aggregation error should be recognized for any statistical testing or assumptions made regarding the local attributes of risk.

The utility of this application is multi-faceted and supports expansion of the original PRISM framework to include more localized vulnerability and risk analyses. In addition to effectively scaling proportional hazard exposures to census tracts, this application of the PRISM framework modifies exposed characteristics to demonstrate how vulnerability and risk calculations for communities can be expanded. The results of this application show that it is possible to assess the potential impacts of multiple hazard exposures at a level comparable to neighbourhoods and use this information to further examine locations and drivers of vulnerability and risk. Coupled with other measures of community health, well-being and resilience, this index could reveal important connections between hazard exposures and socioeconomic characteristics of a community in addition to providing valuable information for mitigation planning.

Disclosure statement

No potential conflict of interest was reported by the authors.

References

Batista MJ, Martins L, Costa C, Relv AM, Schmidt-Thome P, Greiving S, et al. 2004. Preliminary results of a risk assessment study for uranium contamination in central Portugal. Proceedings of the International Workshop on Environmental Contamination from Uranium Production Facilities and Remediation Measures; February 11–13; Lisboa: ITN/DPRSN.

Berke P. 2017. Why is Houston so vulnerable to devastating floods? Boulder (CO): Natural Hazards Center.

Blakie P. and Brookfield H. 1987. Land degradation and society. London: Methuen.

Brooks H. 2004. On the relationship of Tornado path length and width to intensity. Wea Forecast. 19(2):310–319.

Buck KD, Summers KJ, Hafner S, Smith LM, Harwell LC. 2019. Development of a multi-hazard landscape for exposure and risk interpretation: The PRISM approach. Curr Environ Eng. 6(1):74–94.

Burby RJ, Deyle RE, Godschalk DR, Olshansky RB. 2000. Creating hazard resilient communities through land-use planning. Nat Hazards Rev. 1(2):99–106.

Chang SE, Yip JZ, Tse W. 2019. Effects of urban development on future multi-hazard risk: the case of Vancouver. Nat Hazards. 98(1):251–265.

Cheng C, Fotheringham SF. 2013. Multi-scale issues in cross-border comparative analysis. Geoforum. 46:138–148.

Chester DK, Degg M, Duncan AM, Guest JE. 2000. The increasing exposure of cities to the effects of volcanic eruptions: a global survey. Global Environ Change Part B: Environ Hazards. 2(3):89–103.

Cutter SL. 1996. Vulnerability to environmental hazards. Prog Hum Geogr. 20(4):529–539.

Cutter SL, Solecki WD. 1989. The national pattern of airborne toxic releases. Prof Geogr. 41(2):149–161.

Cutter SL, Barnes L, Berry M, Burton C, Evans E, Tate E, Webb J. 2008. A place-based model for understanding community resilience to natural disasters. Global Environ Change. 18(4): 598–606.

Cutter SL, Burton C, Emrich C. 2010. Disaster resilience indicators for benchmarking baseline conditions. J Homel Secur Emerg Manag. 7(1):51–51.

Durham K. 2003. Treating the risks in Cairn. Nat Hazards. 30(2):251–261.

Federal Emergency Management Agency (FEMA 2009a). *Hazus MH MR4 – Flood Model Technical Manual*. Washington, DC: FEMA.

Federal Emergency Management Agency (FEMA). 2009b. National earthquake hazards reduction program recommended seismic provisions for new buildings and other structures (FEMA P-750). Washington (DC): Department of Homeland Security.

Federal Emergency Management Agency (FEMA). 2013. Multi-hazard loss estimation methodology: flood model hazus-MH technical manual. Washington (DC): Department of Homeland Security, Federal Emergency Management Agency Mitigation Division.

Federal Emergency Management Agency (FEMA). 2018. FEMA – Harvey Damage Assessments and Claims, Hydroshare,.

Fleischhauer M, Greiving S, Schlusemann B, Schmidt-Thome P, Kallio H, Tarvainen T. 2005. Multi-risk assessment of spatially relevant hazards in Europe. ESMG symposium, 11–13 October; Nürnberg, Germany: ESPON.

Fotheringham S, Wong D. 1991. The modifiable areal unit problem in multivariate statistical analysis. Environ Plan A. 23(7):1025–1044.

Garschagen M, Romero-Lankao P. 2015. Exploring the relationships between urbanization trends and climate change vulnerability. Clim Change. 133(1):37–52.
Greiving S, Fleischhauer M, Lückenkötter J. 2006. A methodology for an integrated risk assessment of spatially relevant hazards. J Environ Plann Manage. 49(1):1–19.
Güneralp B, Güneralp I, Liu Y. 2015. Changing global patterns of urban exposure to flood and drought hazards. Global Environ Change. 31:217–225.
Hawbaker T, Vanderhoof M, Beal Y, Takacs J, Schmidt G, Falgout J, et al. 2017. Landsat Burned Area Essential Climate Variable products for the conterminous United States (1984–2015). U.S. Geological Survey data release.
Hewitt K, Burton I. 1971. The hazardousness of a place: A regional ecology of damaging events. Toronto: University of Toronto Press.
Hey D, Philippi N. 1995. Flood reduction through wetland restoration: The Upper Mississippi River basin as a case history. Restor Ecol. 3(1):4–17.
Holzer TL, Galloway DL. 2005. Impacts of land subsidence caused by withdrawal of underground fluids in the United States. Humans as Geologic Agents. Vol. 16, Boulder, CO: The Geological Society of America. pp. 87–99.
Homer C, Dewitz J, Yang L, Jin S, Danielson P, Xian G, et al. 2015. Completion of the 2011 National Land Cover Database for the conterminous United States-representing a decade of land cover change information. Photogramm Eng Remote Sens. 81(5):345–354.
Kahn SD. 2005. Urban development and flooding in Houston Texas, inferences from remote sensing data using neural network technique. Environ Geol. 47(8):1120–1127.
Kappes M, Keiler M, Elverfeldt K, Glade T. 2012. Challenges of analyzing multi-hazard risk: a review. Nat Hazards. 64(2):1925–1958.
King P, Beikman H. 1974. Geologic map of the United States (exclusive of Alaska and Hawaii) U.S. Geological Survey, scale 1:2,500,000, 2 sheets.
Lall SV, Deichmann W. 2012. Density and disasters: economics of Urban hazard risk. World Bank Res Obser. 27(1):74–105.
Mileti D. 1999. Disasters by design: a reassessment of natural hazards in the United States. Washington, DC: Joseph Henry Press.
National Weather Service. (NWS 2018). Storm data preparation. Directive National Weather Service Instruction 10-1605. Washington, D.C.: National Weather Service.
National Weather Service (NWS 2016). Severe weather database files (1950–2016). NOAA NWS. http://www.spc.noaa.gov/wcm/#data.
National Drought Mitigation Center (NDMC), U.S. Department of Agriculture (USDA), National Oceanic and Atmospheric Administration (NOAA). 2017. United States Drought Monitor Database. http://droughtmonitor.unl.edu/MapsAndData/GISData.aspx.
O'Keefe J, Beyer-Clow L, Hojnicki J, Goldin H, Welch J. 2006. Forest Preserve and Conservation Districts in Northeastern Illinois: Meeting the Challenges of the 21st Century. Openlands.
Radbruch-Hall, D.H., Colton, R.B., Davies, W.E., Lucchitta, I., Skipp, B.A., and Varnes, D.J.1982. Landslide Overview Map of the Conterminous United States. Geological Survey Professional Paper 1183, U.S. Government Printing Office. Washington, D.C..
Schmidt-Thome P. 2006. ESPON Project 1.3.1 – Natural and technological hazards and risks affecting the spatial development of European regions. Espoo, Finland: Geological Survey of Finland.
Simpson R, Reihl H. 1981. The hurricane and its impact. Baton Rouge and London: Louisiana State University Press.
Spatial Hazard Events and Losses Database for the United States. 2016. *Version 15.2*. Available at: https://cemhs.asu.edu/sheldus/. (Accessed November 14).
Summers JK, Smith LM, Harwell LC, Buck KD. 2018. Measuring community resilience to natural hazards: the natural hazard resilience screening index (NaHRSI)-development and application to the United States. Geohealth. 2(12):372–394..
Tate E, Burton C, Berry M, Emrich C, Cutter SL. 2011. Integrated hazards mapping tool. Trans GIS. 15(5):689–706.

U.S. Census Bureau. 2015. ACS demographic and housing estimates, 2011–2015 American Community survey 5-year estimates. Retrieved from: https://factfinder.census.gov/faces/tableservices/jsf/pages/productview.xhtml?pid=ACS_15_5YR_B04006&prodType=table.

U.S. Geological Survey. 2003. Earthquake Hazards Program: U.S. Seismic Design Maps: U.S. Geological Survey.

U.S. Nuclear Regulatory Committee (USNRC). 2014. Emergency Preparedness at Nuclear Power Plants. www.nrc.gov.

Wahlstrom M, Guha-Sapir D. 2015. The human cost of weather-related disasters 1995–2015. Geneva: United Nations International Strategy for Disaster Reduction.

Weatherford C, Gray W. 1988. Typhoon structure as revealed by aircraft reconnaissance. Part II: Structural variability. Mon Wea Rev. 116(5):1044–1056.

Zhu P. 2008. A multiple scale modeling system for coastal hurricane wind damage mitigation. Nat Hazards. 47(3):577–591.